

On the interpretation of resonance frequencies recorded during microseismic experiments

Jean Baptiste Tary* and Mirko van der Baan, Department of Physics, University of Alberta, Edmonton

tary@ualberta.ca

and

David Eaton, Department of Geoscience, University of Calgary, Calgary

Summary

Continuous passive seismic recordings during hydraulic fracture treatments can be used to map the frequency content of wavefields emitted by microseismic events during fluid injection. Recent studies have shown that the frequency content of continuous recordings contains information on the fluid injection. In particular, spectral lines can be caused by different phenomena leading to similar resonance frequencies. The first step is then to identify and separate the possible sources (receiver, path and source effects) to facilitate the interpretation of the specific resonances due to fluid injection.

We here report two case studies where resonance frequencies are detected. In the case of the first case study, some low-frequency (5-50 Hz) resonance frequencies are found on the borehole geophones as well as two arrays of broadband stations on the surface. The spatial distribution of the stations that have recorded these resonances suggests that they could originate from the vertical and the horizontal parts of the injection well. For the second case study, four spectral lines are detected at 17, 35, 51 and 60 Hz during two stages of the same experiment. Path effects will be limited in this case due to the experimental setup, and the resonance frequencies due to receiver effects are expected to be either higher or lower frequencies. Therefore, the first three resonance frequencies likely result from source effects. The length of a fluid-filled crack resonating at a frequency of 17 Hz is around 17 m. We propose that several interconnected fractures could generate such resonance frequencies. Hence, in this case the resonance frequencies would correspond to mesoscale deformations inside the reservoir, occurring during the fluid injection.

Introduction

Fluid injection to enhance the permeability of tight hydrocarbon reservoirs is often monitored using passive seismic methods. Geophones deployed in one or several observation wells are used to record and locate induced microseismic events. For tight hydrocarbons, the cloud of microseismicity is often assumed to reflect the extension of the part of the reservoir where the permeability and the drainage were enhanced. With this approach, however, only brittle failure is taken into account from the total geomechanical reservoir deformation. This may not present a complete picture, because of the discrepancy between the total energy corresponding to the fluid injection and the energy released by the microseismicity (Maxwell, 2008). Apart from fluid leak-off and fluid friction in the well and the formation, brittle failure is likely not the only type of deformation occurring due to the fluid injection. Other types of deformation such as tensile fracturing or slow deformation may also release part of the “missing” energy.

Apart from triggered events, continuous passive recordings of microseismic experiments and particularly their frequency content may also give valuable information as shown by Pettitt et al. (2009) and Das and Zoback (2012). Das and Zoback (2012) use spectrograms to design a band-pass filter allowing them to detect low-frequency events in continuous recordings. Pettitt et al. (2009) detect

resonance frequencies all along the experiment, correlated with the variations in slurry flow. During one of the injection stages, some microseismicity occur at two depths while the fluid is injected only at the deepest level. The fluid could then have moved from one formation to the other without triggering any seismicity. The frequency content of the continuous recordings displays spectral lines. Moreover, the amplitude of the high frequency component of these lines decreases at the time of the possible inter-level communication. Pettitt et al. (2009) interpret this decrease as the coalescence of micro-fractures, enabling the fluid to move from the deepest formation to the upper one without generating any brittle deformation.

Resonance frequencies can, however, be produced in different ways during microseismic experiments (Tary and van der Baan, 2012) and, in each case, a careful review of all possible causes is necessary (i.e. receiver, path or source sides). In the following we describe two experiments exhibiting resonance frequencies that could result from receiver and source effects.

Methodology - Causes of resonance frequencies

During microseismic experiments, resonance frequencies can be produced at the receiver or source sides, or during waves propagation (Tary and van der Baan, 2012). At the receiver side, resonance frequencies result from the waves reverberations in the borehole (Sun and McMehan, 1988), either the whole borehole or between secondary sources such as the geophones (St-Onge and Eaton, 2011). Resonances can also be due to mechanical resonance of the geophone if its clamping or damping is flawed.

Along the ray path, resonances arise from constructive and destructive interferences of seismic waves, waves focusing in low-velocity waveguides or waves multi-scattering. Which frequency band is favored depends on the layers spacing, thickness and mechanical properties (van der Baan et al., 2007, van der Baan, 2009).

At the source side, resonance frequencies can be generated by repetitive events if perfectly periodic, or by the resonance of fluid-filled cracks as in the case of volcanic tremors (Aki et al., 1977). Resonances in fluid-filled cracks are generated by interface waves and depend mainly on the crack geometry, the crack stiffness and the source parameters that trigger the resonance (Ferrazzini and Aki, 1987).

Results - Case study 1

The first case study corresponds to a microseismic experiment that took place in Northern BC in 2011. During this experiment, 21 stages in two horizontal wells were recorded by 6 downhole geophones, and by 21 broadband geophones and 8 short-period geophones on the surface. Apart from the numerous microseismic events, some resonance frequencies were also recorded by the downhole geophones as well as some of the broadband arrays on the surface (Figure 1).

The resonances are mainly in the frequency band between 5 and 20 Hz. Other resonances are visible on the broadband recordings. They likely correspond to environmental or anthropogenic noises. Noticeably, the resonances were recorded by the downhole geophones, which are close to the horizontal part of the injection well at depth, and by the broadband arrays A and B, which are near the well head. The broadband arrays C or D, closest to the fluid injection during the first stages, did not exhibit any resonance frequencies. This indicates that the injection well is likely the cause of these resonance frequencies.

Results - Case study 2

The second case study is a two-stage microseismic experiment recorded by 12 downhole geophones. During the two stages, most of the geophones show clear resonance frequencies at 17, 35, 51 and 60 Hz (Figure 2). Except for the one 60 Hz which corresponds to the electric current, the others seem to be harmonics of the resonance at 17 Hz.

During this experiment, the length of the borehole is roughly 2300 m and the P-wave velocity in the cement casing is around 3800 m/s, leading to a borehole resonance frequency of ~ 1.7 Hz. The spacing of the geophones is 10.4 m, giving a resonance of ~ 365 Hz (St-Onge and Eaton, 2011). These resonances are then too low or too high to explain the observed resonances. The perforations, as well as the microseismicity occur at around the same depth as those of the receivers. Wave propagation is then predominantly horizontal in this configuration and path effects on the wavetrain will be limited.

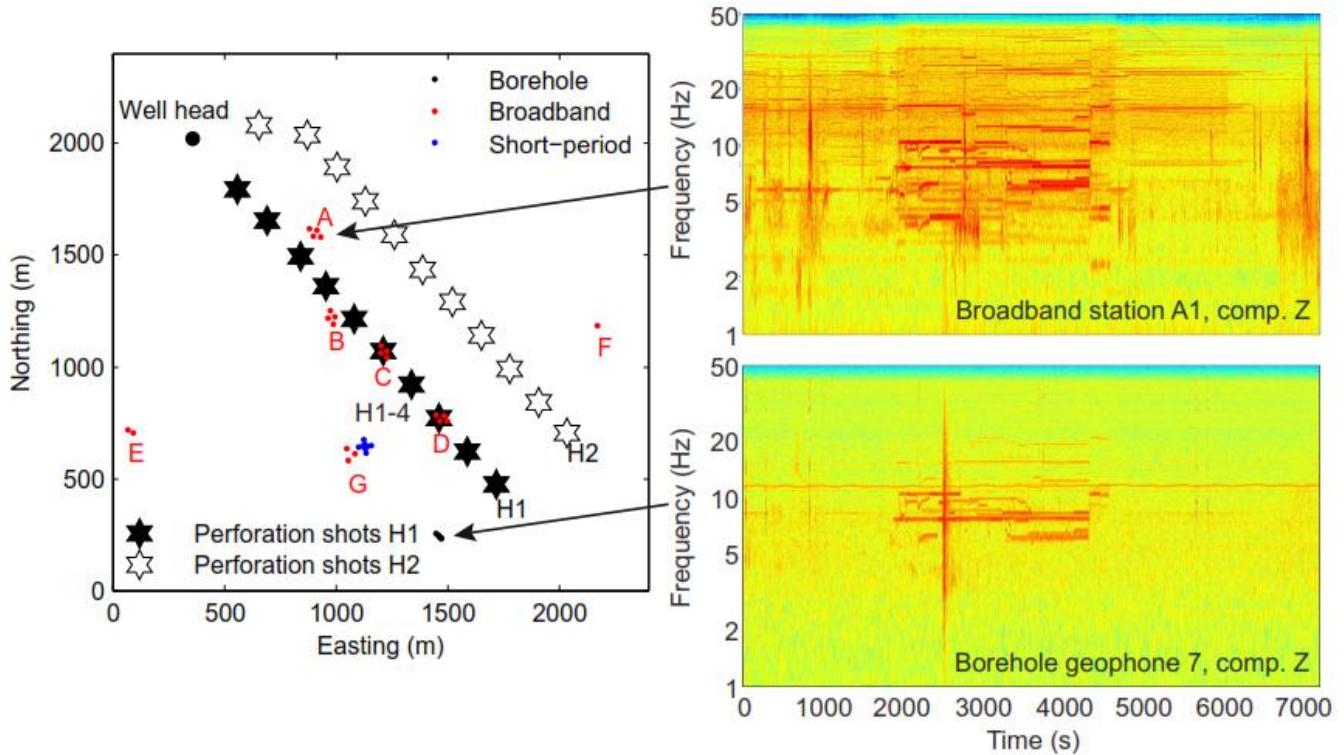


Figure 1. Experimental setup of the first experiment, as well as the time-frequency transforms of stage H1-4 for one downhole geophone and one broadband station (hot colors correspond to high amplitudes). The stars indicate the position of the perforation shots and hence of the horizontal part of the wells. H1 and H2 are two different horizontal wells.

In this case, source effects are more likely. Using the relationship of Korneev (2008) relating the dimension of a fracture to its resonance frequency, a 17 Hz-resonance would correspond to a 17 m-long and 0.005 m-thick fracture. Typical microseismic events with magnitudes between -3 and -1 have crack radii between ~ 0.25 and ~ 2 m (Brune, 1970). The observed resonances could then correspond to a network of several interconnected fractures (Tary and van der Baan, 2012).

Conclusions

The noise amplitude of passive microseismic recordings as well as the frequency content may be correlated to the deformation caused by the fluid injection. Time-frequency transforms can be used to detect changes in frequency content, such as the appearance/disappearance of spectral lines. During two experiments, some resonance frequencies were identified in the lower part of the frequency spectrum (0-60 Hz). Differences in frequency content between experiments shows that, depending on the whole experimental setup and in situ rocks properties, different processes may occur. Hence, in each case, a detailed review of the possible sources of resonance frequencies at the receiver, path and source sides is necessary. Nevertheless, detection of resonances is limited to the bandwidth of the geophones employed in microseismic experiments. Typically, these geophones have a lower bound

around 3-5 Hz, which is greater than some of the expected frequency of low-frequency phenomena that have been documented in volcanic environment or at plate boundaries indicative of slow (aseismic) deformation (0.1-10 Hz).

For the second case study, resonance frequencies are likely associated to source effects. These resonances could correspond to mesoscale deformation taking place inside the reservoir, lying in between the total stimulated rock volume and the individual microseismic events. This shows that a careful study of the frequency content of passive microseismic recordings may improve our understanding of low-frequency process occurring inside the reservoir, potentially associated with aseismic deformation.

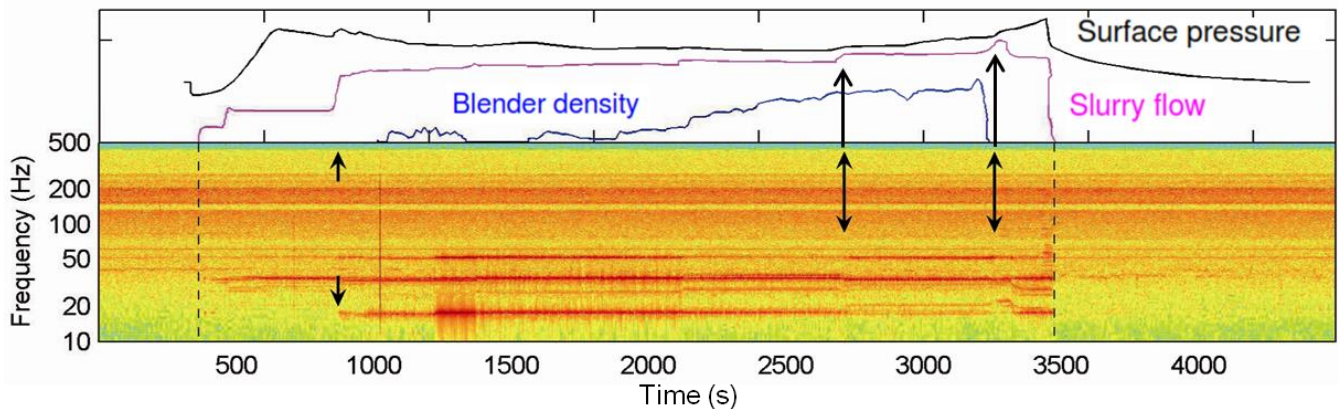


Figure 2. Treatment curve of the first stage of the microseismic experiment of the 2nd case study, as well as the time-frequency transform of the deepest downhole geophone (vertical component). The black arrows indicate some variations in the frequency content that are correlated with changes in the treatment conditions.

Acknowledgements

The authors thank the sponsors of the Microseismic Industry Consortium for financial support, and an anonymous company for permission to show and use their data. Arc Resources, Nanometrics and ESG Solutions are particularly thanked for their support of the field project of the first experiment.

References

- Aki, K., Fehler, M., and Das, S., 1977, Source mechanism of volcanic tremors: fluid-driven crack model and their application to the 1963 Kilauea eruption: *Journal of Volcanology and Geothermal Research*, **2**, 259–287.
- Brune, J., 1970, Tectonic stress and the spectra of seismic shear waves from earthquakes, *Journal of Geophysical Research*, **75**, 4997-5009.
- Das, I., and Zoback, M. D., 2012, Microearthquakes Associated with Long Period, Long Duration Seismic Events During Stimulation of a Shale Gas Reservoir, *SEG Technical Program Expanded Abstracts*, pp. 1-5.
- Ferrazzini, V., and Aki, K., 1987, Slow waves trapped in a fluid-filled infinite crack: implication for volcanic tremor, *Journal of Geophysical Research*, **92**(B9), 9215-9223.
- Korneev, V., 2008, Slow waves in fractures filled with viscous fluid, *Geophysics*, **73**, N1-N7.
- Maxwell, S. C., Shemeta, J., Campbell, E., and Quirk, D., 2008, Microseismic Deformation Rate Monitoring, *Annual Technical Conference and Exhibition, Society of Petroleum Engineers*, SPE 116596.
- Pettitt, W., Reyes-montes, J., Hemmings, B., Hughes, E., and Young, R. P., 2009, Using Continuous Microseismic Records for Hydrofracture Diagnostics and Mechanics, *SEG Expanded Abstract*, **28**, 1542–1546.
- St-Onge, A., and Eaton, D., 2011, Noise Examples from Two Microseismic Datasets, *CSEG Recorder*, **36**, 46-49.
- Sun, R., and McMeahan, G., 1988, Finite-Difference Modeling of Borehole Resonances: *Energy Resources*, **10**, 55-75.
- Tary, J., and van der Baan, M., 2012, Potential use of resonance frequencies in microseismic interpretation, *The Leading Edge*, **31**, 1338-1346.

- van der Baan, M., 2009, The origin of SH-wave resonance frequencies in sedimentary layers, *Geophysical Journal International*, **178**, 1587-1596.
- van der Baan, M., Wookey, J., and Smit, D., 2007, Stratigraphic filtering and source penetration depth, *Geophysical Prospecting*, **55**, 679-684.